

Analysis of the Spatial Sensitivity of Conductance / Admittance Catheter Ventricular Volume Estimation

Erik R. Larson, Marc D. Feldman, Jonathan W. Valvano, *Member, IEEE*, and John A. Pearce, *Senior Member, IEEE*

Abstract— Conductance catheters are known to have a nonuniform spatial sensitivity due to the distribution of the electric field. The Geselowitz relation is applied to murine and multi-segment conductance catheters using finite element models to determine the spatial sensitivity in a uniform medium and simplified left ventricle models. A new formulation is proposed that allows determination of the spatial sensitivity to admittance.

Analysis of FEM numerical modeling results using the Geselowitz relation provides a true measure of parallel conductance in simplified left ventricle models for assessment of the admittance method and hypertonic saline techniques. The spatial sensitivity of blood conductance (G_b) is determined throughout the cardiac cycle. G_b is converted to volume using Wei's equation to determine if the presence of myocardium alters the nonlinear relationship through changes to the electric field.

Results show that muscle conductance (G_m) from the admittance method matches results from the Geselowitz relation, and that the relationship between G_b and volume is accurately fit using Wei's equation. Single-segment admittance measurements in large animals result in a more evenly distributed sensitivity to the LV blood pool. The hypertonic saline method overestimates parallel conductance throughout the cardiac cycle in both murine and multi-segment conductance catheters.

Index Terms—tetrapolar, conductivity, permittivity, sensitivity, conductance catheter

I. INTRODUCTION

BIOIMPEDANCE measurements are often used to indirectly monitor physiologic processes such as blood volume. The conductance catheter technique was introduced by Baan [1] as a method to continuously measure left ventricle (LV) volume. The technique places a multi-electrode catheter

Manuscript received March 14 2013. This work was supported in part by the T.L.L. Temple Foundation and The South Texas Veterans Health Care System, San Antonio, Texas.

E. R. Larson was with the Department of Electrical and Computer Engineering, The University of Texas at Austin, Austin, TX 78712. He is now with Windmill Cardiovascular Systems (email: Larson@ece.utexas.edu)

M. D. Feldman is with the Division of Cardiology, The University of Texas Health Science Center at San Antonio, San Antonio, TX and the Department of Veterans Affairs, South Texas Veterans Health Care System, San Antonio, TX. (email: feldmanm@uthscsa.edu)

J. W. Valvano and J. A. Pearce are with the Department of Electrical and Computer Engineering, The University of Texas at Austin, Austin, TX 78712 USA (e-mail: valvano@mail.utexas.edu; jpearce@mail.utexas.edu).

in the LV and measures the conductance in a tetrapolar configuration. Since the resulting conductance cannot be directly converted to volume, stroke volume estimates are used in the conversion of conductance to volume.

Blood, muscle, and surrounding tissues are included in the conductance measurement as the electric field extends outside the LV blood pool [2, 3]. Conductance outside the LV blood pool, referred to as parallel conductance, causes error in the volume estimation.

Plethysmography instruments commonly measure the magnitude of impedance, neglecting the complex nature of tissues. Cardiac and skeletal muscle exhibit significant permittivity at frequencies above 2 kHz [4, 5] and are an important consideration in plethysmography measurements.

Muscle's high permittivity is most likely due to the transmembrane charge distribution. Charge is held by electrostatic forces across the membrane and forms a dipole which reacts to the application of electric fields.

Two techniques are commonly used to remove parallel conductance: the hypertonic saline method [6] and the admittance method [2, 7].

The hypertonic saline technique injects a small saline bolus into the right heart. As the bolus enters the LV, the high conductivity increases the measured conductance from the LV catheter while the SV is unchanged. End-diastolic (ED) and end-systolic (ES) conductance are used to project the parallel conductance from a linear fit.

The admittance method uses the complex nature of muscle to remove parallel conductance. Measured admittance consists of three components, $\mathbf{Y} = G_b + G_m + j\omega C_m$, where G_b is the conductance of blood, G_m is the conductance of muscle and ωC_m is the susceptance of muscle. Since the imaginary component arises solely from the muscle, the conductivity to permittivity ratio of muscle can be used to separate blood conductance by the conductance-capacitance analogy, $G_b = \text{Re}\{\mathbf{Y}\} - (\sigma_m/\epsilon_m)\text{Im}\{\mathbf{Y}\}$.

Finite element analysis of conductance measurements are normally performed through calculation of total impedance only, ignoring the spatial sensitivity of the measurement. Tetrapolar measurements exhibit intricate sensitivity fields due to separation of the current carrying and voltage sensing electrodes. This work examines the spatial sensitivity of

admittance measurements performed using single- and multi-segment conductance catheters.

II. METHODS

A. Conductance-Capacitance Analogy and the Impedance Formulation

Electrical properties are commonly defined with respect to a bulk measurement. A medium with finite conductivity and permittivity is modeled as a parallel resistor-capacitor network. Electric conductance, G , and capacitance, C , are defined as,

$$G = \frac{I}{V} = \frac{\iint_S \sigma \mathbf{E} \cdot d\mathbf{s}}{\int_b^a \mathbf{E} \cdot d\mathbf{L}} = \sigma F \quad (1)$$

and

$$C = \frac{Q}{V} = \frac{\iint_S \epsilon \mathbf{E} \cdot d\mathbf{s}}{\int_b^a \mathbf{E} \cdot d\mathbf{L}} = \epsilon F, \quad (2)$$

where I is the applied current [A], V is the measured voltage [V], Q is the charge [C], σ is the conductivity [S/m], ϵ is the permittivity [F/m], \mathbf{E} is the electric field [V/m], and F [m] is the field form factor. The surface S is any cross section between the current carrying electrodes and the line integral is any path between the voltage sensing electrodes.

This bulk definition may lead one to incorrectly conclude that the measurement is confined to the region between the equipotential surfaces formed by the voltage sensing electrodes [8]. Property variations between each pair of current-carrying and voltage-sensing electrodes contribute significantly to the total measurement. Another definition of impedance is necessary to quantify spatial contributions to the total measurement.

The relationship between the measured impedance and the local properties in a domain has previously been explored for the tetrapolar measurement [8-10]. Geselowitz formulated a volumetric impedance calculation for plethysmography using the reciprocal nature of the tetrapolar measurement. The Geselowitz relation is a function of two field solutions for an applied source between either the inner or outer electrodes. Lehr developed an alternate derivation allowing non-constant conductivity throughout the volume.

Previous derivations used a volume conductor model. Here we briefly show the derivation for semiconductor dielectrics. We first define a region with finite conductivity, σ , and permittivity, ϵ . Four electrodes are placed on the surface of the medium. The current, I , is applied between terminals A and B which results in the electric potential distribution $\varphi(\mathbf{r})$. Alternatively, applying the same current between electrodes C and D results in the potential distribution $\psi(\mathbf{r})$. The measured impedance is the same under linear conditions due to reciprocity if the current and potential electrodes are swapped. This is only valid for the case where the positive current electrode is swapped with positive voltage electrode and the negative current electrode for the negative voltage electrode.

$$\mathbf{Z} = \frac{\varphi_{AB}}{I} = \frac{\psi_{CD}}{I} \quad (3)$$

This derivation closely follows Lehr's method, only we substitute the combined translational and displacement current densities, $(\sigma + j\omega\epsilon)\mathbf{E}$, rather than only the translational current density, $\sigma\mathbf{E}$. We first substitute $\psi(\sigma + j\omega\epsilon)\mathbf{E}_\varphi$ into the divergence theorem, and work toward a formulation of the measured impedance.

$$\begin{aligned} \iiint_V \psi(\nabla \cdot [(\sigma + j\omega\epsilon)\mathbf{E}_\varphi]) + (\sigma + j\omega\epsilon)\mathbf{E}_\varphi \cdot \nabla\psi \, dv \\ = \oint_S \psi(\sigma + j\omega\epsilon)\mathbf{E}_\varphi \cdot d\mathbf{s} \end{aligned} \quad (4)$$

Since there are no sources within the medium (boundary value problem), $\nabla \cdot [(\sigma + j\omega\epsilon)\mathbf{E}_\varphi] = 0$.

$$\iiint_V (\sigma + j\omega\epsilon)\mathbf{E}_\varphi \cdot \nabla\psi \, dv = \oint_S \psi(\sigma + j\omega\epsilon)\mathbf{E}_\varphi \cdot d\mathbf{s} \quad (5)$$

We can neglect the normal component of the electric field on the surface at all points other than the applied current source. Assuming that the current is supplied by a perfect conductor we are left only with the applied current and potential.

$$\iiint_V (\sigma + j\omega\epsilon)\mathbf{E}_\varphi \cdot \nabla\psi \, dv = \varphi_A I - \varphi_B I = \varphi_{AB} I \quad (6)$$

If we divide both sides of the equation by I^2 and substitute \mathbf{E}_ψ for $\nabla\psi$,

$$\mathbf{Z} = \iiint_V \frac{(\sigma + j\omega\epsilon)\mathbf{E}_\varphi \cdot \mathbf{E}_\psi}{I^2} \, dv = \frac{\varphi_{AB}}{I} \quad (7)$$

We can manipulate this equation to aid its interpretation by formulating it in terms of the combined translational and displacement current densities, \mathbf{J}_φ^* and \mathbf{J}_ψ^* , rather than the electric fields.

$$\mathbf{Z} = \iiint_V \frac{\mathbf{J}_\varphi^* \cdot \mathbf{J}_\psi^*}{(\sigma + j\omega\epsilon)I^2} \, dv \quad (8)$$

This equation reflects the measured impedance as would be observed with a tetrapolar configuration, and can be applied to a domain with nonuniform properties. Local integration of equation (8) only reflect the region's true impedance in domains oriented electrically in series. It is not valid for local integration in parallel or mixed models since only part of the current is located in each domain, but the integration over the entire domain remains valid.

It is best to analyze conductance catheters in terms of admittance, \mathbf{Y} , rather than impedance due to the geometry of the blood and muscle domains. If we multiply equation (8) by \mathbf{Y}^2 the result is,

$$\mathbf{Y} = \iiint_V \frac{\mathbf{J}_\varphi^* \cdot \mathbf{J}_\psi^*}{(\sigma + j\omega\epsilon)V^2} \, dv, \quad (9)$$

where V is the difference in potential between the measurement electrodes.

Blood and muscle conductance were calculated from finite element models using two methods. The first uses the net admittance measurement and the admittance method to separate the blood and muscle conductance, as would be done experimentally [11]. A second method using subdomain integration of the $\text{Re}\{\mathbf{Y}\}$ over blood and muscle subdomains separately provides an additional method to calculate blood and muscle conductance. The resulting values of each method are compared.

Blood conductance can be converted to volume using Wei's equation [13]. Finite element models were previously used to validate Wei's equation in saline surrounded by an insulating cylinder. Models in this work are used to analyze Wei's equation in the presence of LV muscle.

B. Finite Element Models

Finite element models were created in COMSOL Multiphysics using the electric currents module. The governing equations for this module using a source-free medium are

$$\mathbf{J} = ((\sigma + j\omega\epsilon)\nabla V) \quad (10)$$

and

$$\nabla \cdot \mathbf{J} = 0. \quad (11)$$

Each model contains a tetrapolar electrode array. One electrode is connected to a current source of $10\mu\text{A}_{\text{RMS}}$ at 20 kHz using the boundary condition,

$$\iint_{S1} -\mathbf{n} \cdot \mathbf{J} dS = I, \quad (12)$$

where $S1$ is the electrode surface, \mathbf{n} is the surface normal unit vector, \mathbf{J} is the current density, and I is the applied current. The current sink is set using a constant potential boundary with $V = 0$. Internal boundary conditions are set to

$$\mathbf{n} \cdot (\mathbf{J}_1 - \mathbf{J}_2) = 0, \quad (13)$$

where \mathbf{J}_1 and \mathbf{J}_2 are the current densities at the material interface. The boundary conditions of the surrounding domain are set to electrical insulation,

$$-\mathbf{n} \cdot \mathbf{J} = 0. \quad (14)$$

1) Single-segment Murine Catheter

A tetrapolar murine catheter was first analyzed in a uniform medium to determine the distribution of the sensitivity field. Catheter dimensions were set to match the standard 1.2 F Scisense (London, Ontario) mouse catheter with a segment length of 4.5 mm.

The catheter was placed in a simple cylindrical model of the murine left ventricle. A simple geometry was used in order to aid interpretation of results for this new analysis method. Dimensions of the mouse LV were based on ultrasound measurements [14]. The outer muscle wall dimensions are held constant and the radius of the blood cylinder is varied to simulate volumes throughout the cardiac cycle. Calculations

of blood conductance (G_b) using the admittance method and the Geselowitz relationship are compared, and G_b is converted to volume using Wei's equation.

Hypertonic-saline injection was simulated by varying blood conductivity at end-systole and end-diastole. Blood conductance was increased by approximately 10% to match results from Baan [6].

Analysis of the sensitivity distribution in the blood cavity is performed through computation of the contribution each segmental volume makes to $\text{Re}\{\mathbf{Y}\}$ and G_b . This is performed by integrating over 24 cylinders with a radius that extends to the LV endocardium and a thickness of 0.25 mm.

Surroundings' effect on admittance measurements were studied by adding a larger cylinder around the simplified LV model. The Geselowitz method and the admittance method were again compared and Wei's equation was used to fit the results. The admittance method is unable to remove the contribution of the surroundings to the measured conductance since it has negligible permittivity. A new correction method was used that assumes knowledge of the true end-diastole and end-systolic volumes, which requires the use of ultrasound experimentally. The method corrects for surrounding conductance, G_s , by iteratively determining a constant value of G_s to subtract from G_b that minimizes error in the fit by Wei's equation at end-diastole and end-systole.

Nominal murine subdomain properties are shown in Table I. Blood and muscle properties were used from measurements by Raghavan *et al.* [4]. A value of 0.1 S/m is used for the surroundings, based on lung measurements [15]. Individual surrounding tissues are not modeled.

This simplified model uses isotropic muscle properties. *In-vivo* cardiac properties exhibit anisotropy and are subject to variation from conditions such as myocardial infarction and hypertrophy. Variations in muscle properties affect the ability of the admittance method to remove parallel conductance in these regions.

Previous investigators used power deposition as a surrogate for parallel conductance [3]. The admittance method is compared to the resistive losses in the surroundings calculated as the volume integral over the domain of interest,

$$\text{Resistive Losses} = \iiint \text{Re}\{\mathbf{E} \cdot \mathbf{J}\} dv. \quad (15)$$

Since various tissues actually surround the heart, a parametric sweep is performed from 0.05 S/m to 0.4 S/m to determine the effect of the surrounding's conductivity on resistive losses outside the LV. This range of conductivities was chosen to cover the range of tissue properties surrounding the heart.

Table I
Murine Subdomain Properties

Subdomain	Conductivity (S/m)	Relative Permittivity
Blood	0.46	80
Muscle	0.16	11,800
Surroundings	0.10	80
Catheter (polyimide)	10^{-12}	2

2) Multi-segment Large Animal Catheter

A five-segment conductance catheter was analyzed in a uniform medium to determine the effects of multiple segments on the distribution of the sensitivity field. Each segment's sensitivity field was summed to produce the net sensitivity, according to the traditional conductance catheter method [1].

The catheter dimensions for this study are based on Scisense Systems Inc. (London, Ontario) multi-segment catheters with 10 mm spacing between electrodes except the most distal electrodes, which are spaced at 5 mm.

Further analysis of the five-segment catheter was performed by comparing single- and multi-segment measurements in a cylindrical large animal LV model. Conductivity and permittivity were set based on epicardial surface probe measurements in pigs [16], shown in Table II. Parallel conductance is determined using the admittance method, Geselowitz relation, and the hypertonic saline method.

The sensitivity distribution along the multi-segment catheter is determined through integration over 29 cylinders with a radius that extends to the myocardium and a thickness of 2.5 mm.

Table II
Large Animal Subdomain Properties

Subdomain	Conductivity (S/m)	Relative Permittivity
Blood	0.80	80
Muscle	0.33	19,700
Catheter (polyimide)	10^{-12}	2

III. RESULTS

A. Murine Catheter without Surroundings

1) Uniform medium

Analysis of the mouse catheter in a uniform medium is shown in Fig. 1. This model shows that the measurement is heavily weighted toward the regions in close proximity to the electrodes. Small negative sensitivity fields are located in the regions between the pairs of current-carrying and voltage-sensing electrodes, where $\mathbf{J}_\varphi^* \cdot \mathbf{J}_\psi^*$ results in a negative number. This occurs near the electrodes, where the current densities are oriented in opposing directions. Increases in admittivity in a positive zone increase the measured admittance while increases in a negative zone decrease the measured admittance. One can rationalize negative sensitivity by considering two limit cases. If the impedance between the current-carrying and voltage-sensing electrodes were to drop to zero, then all the current would be directed towards the voltage-sensing electrode causing an increase in the voltage sensed at the voltage-sensing electrode. Similarly, if the impedance between the current-carrying and voltage-sensing electrodes were to increase to infinity, then none of the current would be directed towards the voltage-sensing electrode causing a decrease in the voltage sensed at the voltage-sensing electrode.

2) Simple Murine Left Ventricle Geometry

The resulting geometry of the mouse LV is shown in Fig. 2 at diastole. Systole corresponded to a volume of 15 μL and diastole to 45 μL . Further analysis was performed over a range of 15 to 60 μL .

Comparison of the Geselowitz and admittance method results in Table III show that the real part of the integration of the admittance formulation of the Geselowitz relation, equation (8), over the blood domain is nearly equal to the G_b from the admittance method, as in

$$\text{Re} \left\{ \iiint_{\text{LV blood}} \frac{\mathbf{J}_\varphi^* \cdot \mathbf{J}_\psi^*}{(\sigma + j\omega\epsilon)V^2} dv \right\} = G_b. \quad (16)$$

Hypertonic saline simulations result in a least squares fit to the end-systolic and end-diastolic conductance of $G_{\text{ES}}(\mu\text{S}) = 0.440 \cdot G_{\text{ED}} + 265$, with $R^2 = 0.99999$. This results in a parallel conductance of 473 μS , which is larger than the true parallel conductance determined by the admittance and Geselowitz methods.

The impedivity-sensitivity product, integrand in equation (9), in the mouse LV is shown at 15 μL in Fig. 3 to visually emphasize the removal of muscle using the admittance method. Prior to removal of the muscle signal, the muscle domain clearly contributes to the measurement. Following removal using the admittance method, the contribution of the muscle domain is reduced by 80%.

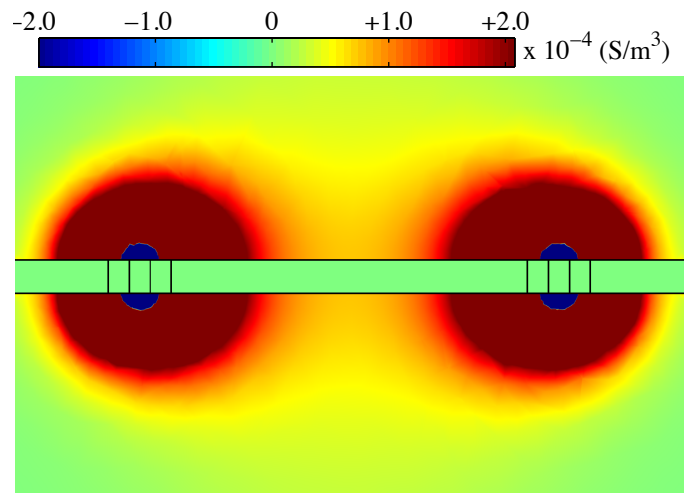


Fig. 1. Spatial contributions are shown by plotting the integrand of equation (9) for the mouse catheter in a uniform medium with a conductivity of 0.46 S/m. Four electrodes are shown along the catheter and are used for the tetrapolar measurement. The largest contributions are in close proximity to the electrodes.

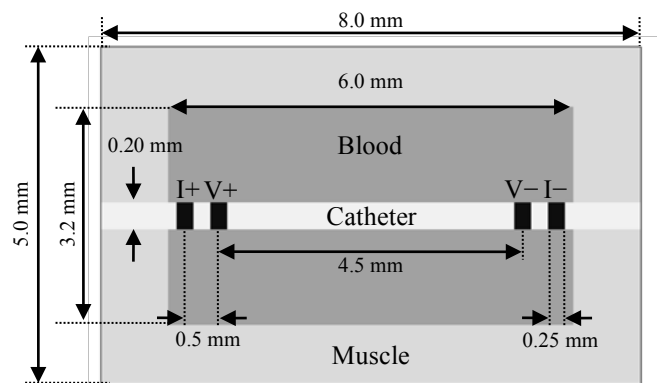


Fig. 2. Mouse conductance catheter in a cylindrical model of the mouse LV at 45 μL (end-diastole). This simplified geometry is used to aid interpretation of analysis using the Geselowitz relation. The diameter of the blood pool was varied to simulate the cardiac cycle.

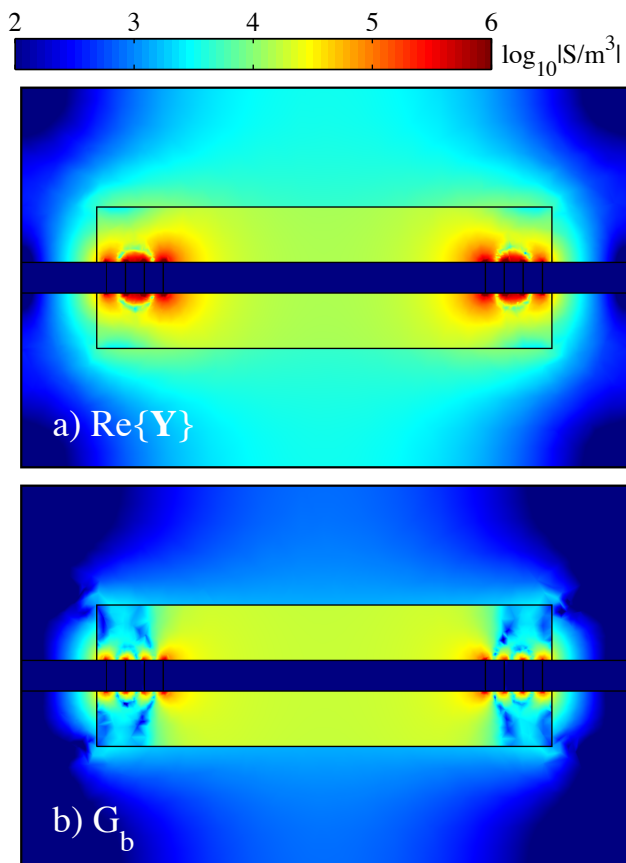


Fig. 3. a) The product of impedivity and sensitivity and b) the product of G_b and sensitivity are shown on log scales. These plots are shown at systole to emphasize the diminished sensitivity to the myocardium using the admittance method. The contribution from the myocardium domain is reduced by 80% at end-systole and by 89% at end-diastole. Sensitivity to the blood pool is decreased near the current carrying electrodes and increased between the voltage sensing electrodes.

The distribution of contributions within the LV blood pool is affected by the admittance method due to the blood and muscle not being perfectly in parallel. Contributions from the segmental blood volumes within 0.75 mm of either electrode are reduced by 56% at end-systole and 10% at end-diastole. Contributions between the electrodes, within ± 1.5 mm, are increased by 18% at end-systole and 8% at end-diastole. A negative sensitivity zone for $\text{Im}\{Z\}$ between the electrodes in the LV blood pool is responsible for the increase in contributions from blood.

Relative contributions to $\text{Re}\{Y\}$ and G_b of each segmental volume in the blood pool are shown in Fig. 4. As expected, the greatest sensitivity is located near the electrodes. Contributions to $\text{Re}\{Y\}$ from subvolumes at least 0.5 mm away from the electrodes are comparable. Sensitivity to G_b is more uniformly distributed, but varies more than $\text{Re}\{Y\}$ with the cardiac cycle.

Volume vs. G_b is plotted in Fig. 5. Points correspond to the data from Table III and the line is Wei's equation calibrated using the 15 μL , end-systole, and 45 μL , end-diastole, data points. The close fit to the model data shows that the nonlinear relationship with volume is unaffected by the admittance method.

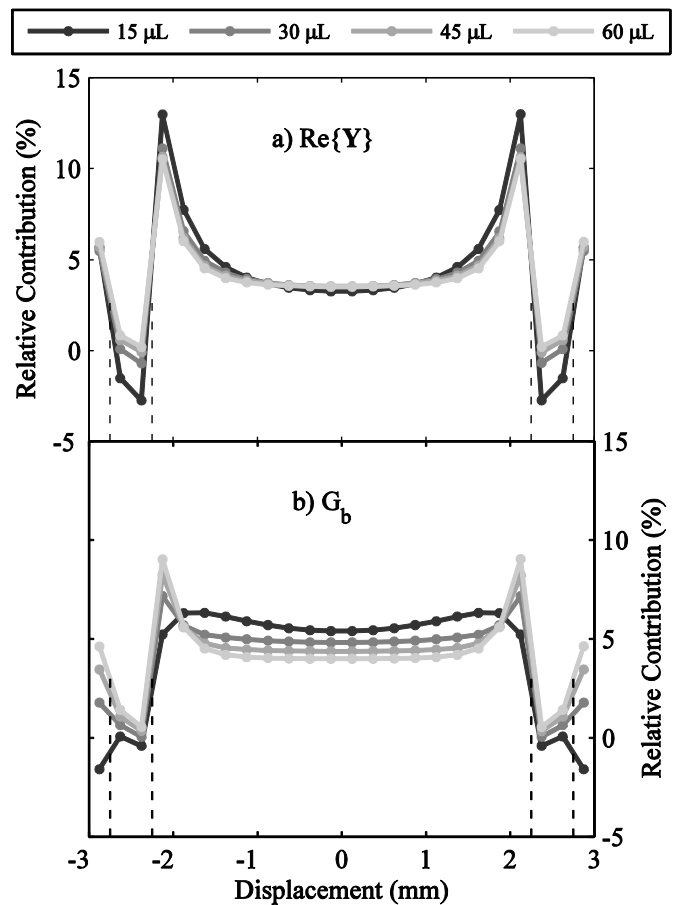


Fig. 4. Relative contributions to a) $\text{Re}\{Y\}$ vs. displacement and b) G_b vs. displacement. Each point corresponds to the integration over a cylinder with a radius equal to the blood pool and a height of 0.25 mm, swept across the long axis of the LV. Dashed lines indicate electrode locations. This shows the nonuniform distribution of sensitivity in the LV. The greatest contributions are located in close proximity to the electrodes. The distribution for $\text{Re}\{Y\}$ shows a large increase in sensitivity near the electrodes whereas the distribution for G_b shows reduced intensity near the electrodes, resulting in a more uniformly distributed sensitivity.

Table III
Mouse Model Results

Volume (μL)	G_b (μS)		G_m (μS)	
	Admittance Method ¹	Geselowitz Relation ²	Admittance Method ¹	Geselowitz Relation ²
15	298.4	298.7	344.6	344.3
30	517.8	518.7	260.8	259.9
45	680.7	682.1	194.3	192.8
60	807.3	809.1	143.7	141.9

Simplified mouse LV model results showing that blood conductance (G_b) from the Geselowitz relation is nearly equal to G_b from the admittance method.

1. Blood conductance (G_b) and muscle conductance (G_m) from the admittance method are calculated using the total admittance from all subdomains.
2. Blood and muscle conductance from the Geselowitz relation are calculated using subdomain integration of equation (8).

3) Simple Murine LV Geometry with Surroundings

The addition of a surrounding medium introduces error into G_b calculated using the admittance method, as it can only remove the muscle component, G_m , of the signal. Calculation results for the Geselowitz and admittance method are shown in Table IV. Following removal of G_m , the admittance method

results in the sum of blood and surrounding conductance. The the surroundings conductance, G_s , from the Geselowitz method varied from 150.7 to 168.3 μS , compared to G_b which varied from 372.7 to 887 μS .

Table IV
Mouse Model Results with Surroundings

Volume (μL)	G_b (μS)		G_s (μS)	G_m (μS)	
	Admittance Method ¹	Geselowitz Relation ²	Geselowitz Relation ²	Admittance Method ¹	Geselowitz Relation ²
15	521.6	372.7	150.7	395.5	393.6
30	783.7	617.2	169.4	288.5	285.7
45	943.6	775.3	171.6	218.1	214.7
60	1051.5	887.0	168.3	171.5	167.7

Simplified mouse LV with surrounding medium results show blood conductance (G_b) from the admittance method is nearly equal to the sum of G_b and surrounding conductance (G_s) from the Geselowitz relation.

1. Blood conductance (G_b) and muscle conductance (G_m) from the admittance method are calculated using the total admittance from all subdomains.
2. Blood conductance (G_b), muscle conductance (G_m), and surrounding conductance (G_s) from the Geselowitz relation are calculated using subdomain integration of equation (8).

Hypertonic saline simulations with the addition of a surrounding medium resulted in a least squares fit to the end-systolic and end-diastolic conductance of $G_{ES}(\mu\text{S}) = 0.479 \cdot G_{ED} + 368$, with $R^2 = 0.99995$. The estimated parallel conductance is 706 μS , much larger than the sum of muscle and surrounding conductance at any point in the cardiac cycle.

Application of Wei's equation to G_b from the admittance method is shown in Fig. 6. The uncorrected G_b that includes the surroundings' conductance, $G - G_m$, overestimates volume by approximately 5 to 7 μL . An estimate for the surrounding conductance is found by adjusting the correction for G_s to produce the best fit to the two calibration points, resulting in a value of 122 μS . This underestimates the true G_s throughout the cardiac cycle, but provides the best fit using a constant value. The corrected blood conductance, $G - (G_m + G_s)$, is more closely fit by Wei's equation.

Resistive losses from the parametric sweep over the surroundings' conductivity are shown in Table V and range from 3.8 to 7.7 percent. The Geselowitz method shows that the relative contribution to the total conductance is higher, and varied from 14 to 16 percent with a conductivity of 0.1 S/m in the surroundings.

Table V
Resistive Losses in Surroundings (% Total Losses)

Surroundings Conductivity (S/m)	Volume (μL)			
	15	30	45	60
0.05	4.7	5.4	6.3	7.4
0.1	5.4	6.0	6.7	7.7
0.2	5.0	5.4	5.8	6.5
0.3	4.3	4.6	4.9	5.4
0.4	3.8	4.0	4.2	4.6

Resistive losses in the surroundings relative to the total losses show values ranging from 3.8 to 7.7 percent, depending on the surrounding conductivity. These values are 2 to 3 times less than the relative contribution of the surroundings to the total admittance, demonstrating that resistive losses can underestimate the contribution to the measurement.

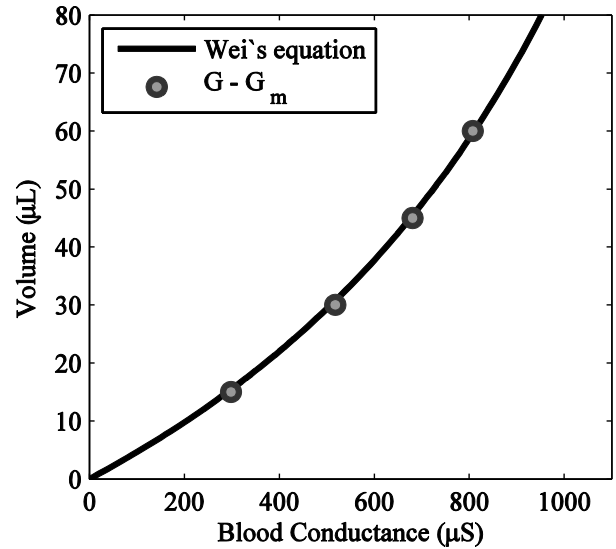


Fig. 5. Wei's equation fit to the blood conductance data from the mouse catheter with no surroundings. Calibration is applied using the SV and blood conductance data between 15 and 60 μL . The fit includes the origin and each G_b measurements from the model, showing that the nonlinear relationship is unaffected by the admittance method.

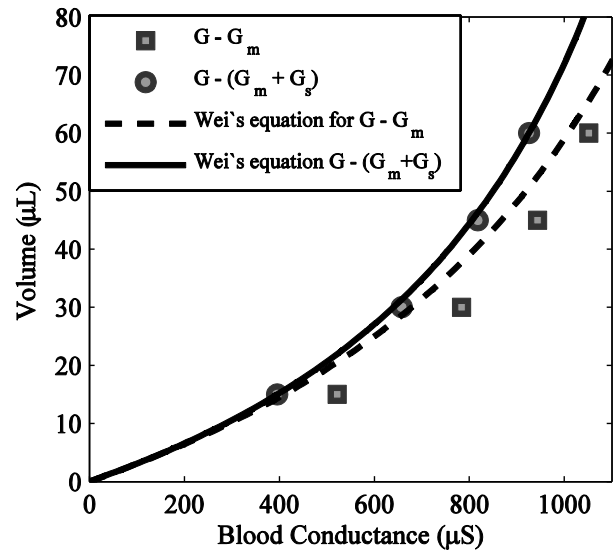


Fig. 6. Wei's equation fit to the blood conductance data from the mouse model with surroundings shows increased accuracy after the estimated surrounding conductance is removed.

B. Multi-segment Catheter

1) Multi-segment catheter sensitivity in a uniform medium

The sensitivity field of each individual segment is shown in Fig. 7. Although these five conductance signals are electrically in series, Baan sums them directly, as each represents a volume signal. The sum of the five conductance measurements is shown in Fig. 7f, and the result of a single-segment measurement across the outermost electrodes is shown in Fig. 7g. While the single-segment sensitivity is weighted heavily towards the outermost electrodes, the multi-segment sensitivity is more evenly distributed but has additional negative sensitivity zones.

2) Multi-segment catheter in a simple LV model

Blood and muscle conductance calculated with the

admittance method and the Geselowitz relation were determined for both single- and multi-segment configurations and both were well fit by Wei's equation. Spatial contributions to $\text{Re}\{\mathbf{Y}\}$ and G_b in the multi-segment configuration are shown in Fig. 8, demonstrating the ability of the admittance method to suppress signal contributions from the myocardium.

Hypertonic-saline simulations for the multi-segment configuration resulted in a least squares fit to the end-systolic and end-diastolic conductance of $G_{ES}(\text{mS}) = 0.557 \cdot G_{ED} + 137$, with $R^2 > 0.99999$. The estimated parallel conductance for the multi-segment measurement was 309 mS. This value is more than double the parallel conductance from the admittance method and Geselowitz relation; they varied from 86 mS at end-diastole to 129 mS at end-systole.

Hypertonic-saline simulations for the single-segment measurement also overestimated parallel conductance at 11.8 mS, where the admittance method and Geselowitz relation resulted in a value of 2.9 mS at end-diastole and 4.5 mS at end-systole.

3) Relative volume contribution

Segmental volume sensitivity results are shown as relative contributions in Fig. 9. Single-segment results are similar to murine catheter results, showing peaks at both ends of the catheter. This result is not symmetric due to a shorter spacing between the stimulating and sensing pair at the distal end of the catheter. Closer spacing produces a larger positive sensitivity region near the stimulating and sensing pair.

Multi-segment segmental volume sensitivity results show a reduction in the peak sensitivity at the distal end of the catheter and an increase in the sensitivity of volume segments in the middle. Sensitivity to G_b is more uniformly distributed in both single- and multi-segment configurations.

IV. DISCUSSION

The major findings of this study are summarized in Table VI. In all models the admittance method correctly removes parallel conductance from the muscle, and results in a more uniform sensitivity distribution in the LV blood pool. The hypertonic saline method overestimates parallel conductance in each model.

A. Murine catheter

Spatial sensitivity analysis of the admittance method was performed using the Geselowitz relation reformulated for complex media. The murine conductance catheter exhibits the highest sensitivity near the stimulating and sensing electrodes. Negative sensitivity zones exist between each pair of stimulating and sensing electrodes, which means that an increase in local electrical conductivity reflects as a decrease in the measured conductance.

The removal of the muscle component from the spatial sensitivity in Fig. 3 results in a reduction in contributions inside the LV blood pool near the current-carrying electrodes and an increase in contributions between the voltage-measuring electrodes. A truly parallel model would not contain an imaginary part inside the blood domain. Despite this limitation, the admittance method has a more uniformly

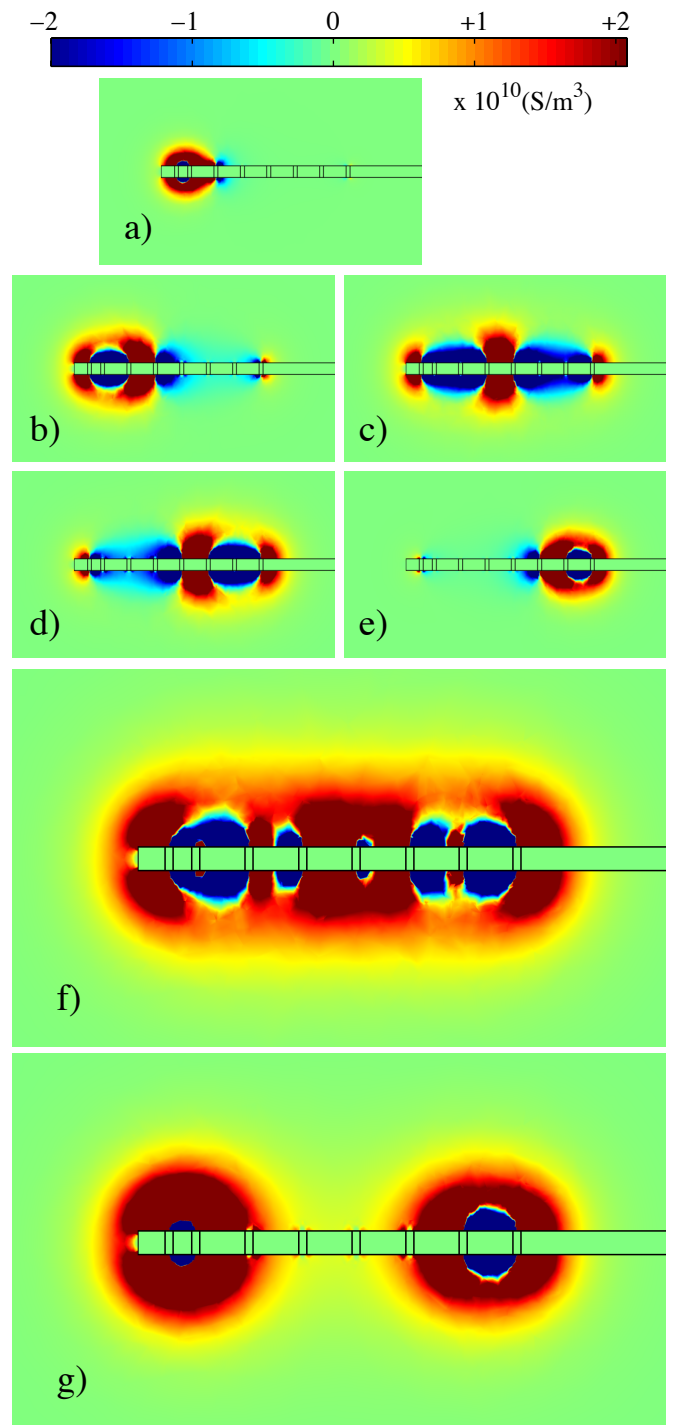


Fig. 7. Spatial contributions in a uniform medium, $\sigma = 0.8 \text{ S/m}$, from a- e) each individual segment, f) combined multi-segment, and g) single-segment. The intensity of the single-segment measurement is scaled such that the magnitude of the measurement matches the multi-segment magnitude. Multi-segment measurements exhibit a more distributed sensitivity along the catheter while the single-segment measurement is concentrated near the measurement electrodes. The catheter radius is 2.2 mm. Electrodes are separated by 10 mm, except the most distal electrode which is separated by 5 mm. Electrodes have a height of 1.5 mm and a radius of 2.2 mm.

distributed spatial sensitivity in the LV chamber than $\text{Re}\{\mathbf{Y}\}$.

Model results show that the admittance method correctly removes parallel conductance and that the hypertonic saline method overestimates parallel conductance throughout the cardiac cycle. This error in parallel conductance estimation

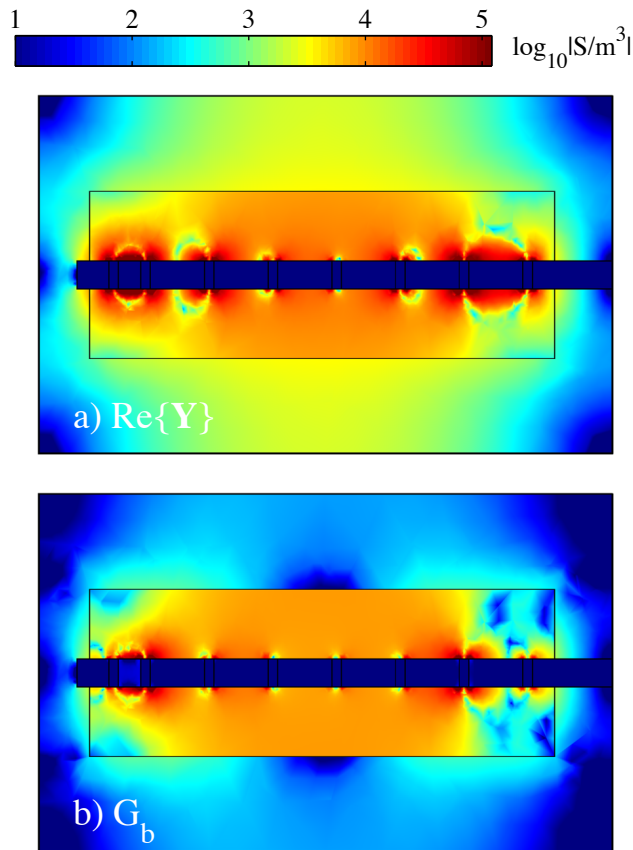


Fig. 8. Multi-segment spatial contributions, configuration from Fig. 7e, plotted on a log scale showing a) distribution for $\text{Re}\{Y\}$ and b) distribution for G_b from the admittance method. Removal of the muscle components of the signal reduces contributions from the muscle domain by 90% at end-systole and end-diastole. Sensitivity to the blood pool is decreased near all electrodes, especially near the outermost electrodes. Sensitivity to the blood pool is increased away from the electrodes between the voltage sensing electrodes. The myocardium has a radius of 28 mm and a height of 90 mm. The blood pool has a radius of 18.5 mm at diastole and a height of 73 mm.

is independent of errors due to changes in LV preload due to the saline bolus [12]. G_b errors using the admittance method are due to the true model being a mixture of parallel and series combinations of blood and muscle. Agreement between G_b from the admittance method and Geselowitz relation shows that a parallel model accurately represents the conductance catheter sensing domains.

Further analysis quantifies the nonlinear sensitivity along the catheter, showing the highest sensitivity to $\text{Re}\{Y\}$ near the electrodes, which does not change significantly over the cardiac cycle. Following the removal of muscle, G_b shows reduced sensitivity near the current-carrying electrodes and enhanced sensitivity between the voltage-measuring electrodes. Changes to the sensitivity distribution between $\text{Re}\{Y\}$ and G_b are due to the model being a mixture of parallel and series combinations of blood and muscle.

Wei's equation correctly fits G_b , showing that the equation is not affected by changes to the field geometry due to the presence of the myocardium.

Results from this study show that resistive losses underestimate the myocardial contribution to conductance by a factor of 2 to 3, and thus power deposition should not be used

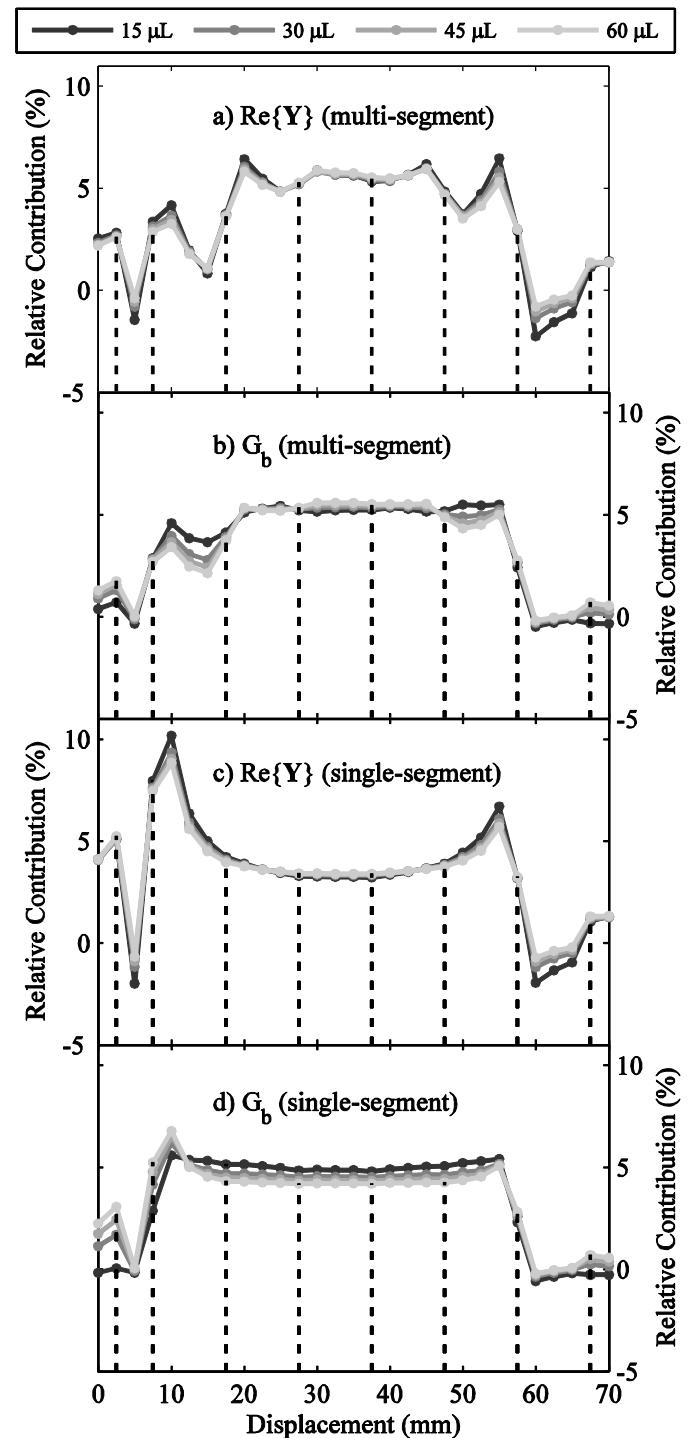


Fig. 9. Relative segmental volume contribution for a) $\text{Re}\{Y\}$ (multi-segment), b) G_b (multi-segment), c) $\text{Re}\{Y\}$ (single-segment), and d) G_b (single-segment). Non-uniform sensitivities are affected by the location of electrodes. Application of the admittance method reduces variations in sensitivity, particularly for the single-segment configuration from Fig. 7g. The distribution of sensitivity using the admittance method is comparable using single-segment with the admittance method and traditional multi-segment catheters with magnitude measurements.

to estimate subdomain signal contributions with tetrapolar measurements.

Table VI
Summary of Results

Simplified mouse model	
Admittance method	Correctly removes G_m
Hypertonic saline	$G_{ } / G_m \geq 1.4$
Sensitivity distribution	G_b more uniform than $\text{Re}\{Y\}$
Simplified mouse model (with surroundings)	
Admittance method	Removes G_m , but not G_s
Hypertonic saline	$G_{ } / (G_m + G_s) \geq 1.3$
Volume conversion	Admittance method overestimates volume by 5 to 7 μL due to G_s
Power deposition	Surrounding losses overestimate G_s by factor of 2-3
Simplified large animal model	
Single-segment	
Admittance method	Correctly removes G_m
Hypertonic saline	$G_{ } / (G_m + G_s) \geq 2.6$
Sensitivity distribution	G_b more uniform than $\text{Re}\{Y\}$ for both single- and multi- segment results
Multi-segment large	
Admittance method	Correctly removes G_m
Hypertonic saline	$G_{ } / (G_m + G_s) \geq 2.4$
Sensitivity distribution	G_b more uniform than $\text{Re}\{Y\}$

Summary of findings where G_m is blood conductance, $G_{||}$ is parallel conductance from the hypertonic saline method, G_b is blood conductance, $\text{Re}\{Y\}$ is the real part of admittance, and G_s is conductance of the surroundings of the heart.

B. Multi-segment catheter

Spatial sensitivity analysis in a simplified LV model shows that the single-segment admittance method results in a more evenly distributed sensitivity in the LV blood pool than multi-segment admittance and $\text{Re}\{Y\}$ in both single- and multi-segment configurations, as shown in Fig. 9. Multi-segment sensitivity analysis shows that each segment exhibits a distribution weighted towards the current-carrying and voltage-sensing electrodes for that particular configuration, as in Fig. 7. Although the sum of multiple segments is more evenly distributed than a single-segment for $\text{Re}\{Y\}$, variability remains due to the concentration of sensitivity near the electrodes along the catheter.

Results show that there is little difference between the single- and multi-segment measurements following conversion to volume, but such differences may be minimized due to the simple geometry of this model. *In vivo* measurements are subject to larger variations in geometry near the apex and base of the ventricle. While these variations affect blood volume, their influence may change the nonlinear relationship between conductance and volume. Models show that the admittance method is able to remove muscle conductance. This work suggests that single-segment admittance measurements may be used in large animals for the first time, while they would not be successful when magnitude only is measured.

V. CONCLUSION

Analysis of conductance catheter measurements using the Geselowitz relation quantifies the nonuniform spatial sensitivity, and allows calculation of contributions from each domain. Muscle conductance calculated using the admittance method matches results from the Geselowitz relation, and the

hypertonic saline method overestimates parallel conductance throughout the cardiac cycle in simplified models of both small and large animal hearts. Analysis shows single-segment measurements in large animals using the admittance method provide a superior sensitivity distribution to the LV blood pool compared to traditional multi-segment measurements in a simplified LV model.

ACKNOWLEDGMENT

The authors would like to thank Dr. John Porterfield for his help with the FEM modeling. This work was funded in part by Scisense Systems Inc., Ontario, Canada. Drs. Feldman, Valvano, and Pearce have a financial interest in Admittance Technologies Inc. All data and calculations in this manuscript are the sole property of the authors and the University of Texas at Austin.

REFERENCES

- [1] J. Baan, J. Koops, E. T. Vandervelde, D. Temmerman, and B. Buis, "Dynamic Absolute Left-Ventricular Volume Measured with the Conductance Catheter," *Circulation*, vol. 64, pp. 177-177, 1981.
- [2] C. L. Wei, J. W. Valvano, M. D. Feldman, M. Nahrendorf, R. Peshock, and J. A. Pearce, "Volume catheter parallel conductance varies between end-systole and end-diastole," *IEEE Transactions on Biomedical Engineering*, vol. 54, pp. 1480-1489, 2007.
- [3] C. Constantinides, S. I. Angeli, and R. J. Mean, "Murine Cardiac Catheterizations and Hemodynamics: On the issue of Parallel Conductance," *IEEE Transactions on Biomedical Engineering*, vol. 58, pp. 3260-3268, Nov 2011.
- [4] K. Raghavan, J. E. Porterfield, A. T. G. Kottam, M. D. Feldman, D. Escobedo, J. W. Valvano, and J. A. Pearce, "Electrical Conductivity and Permittivity of Murine Myocardium," *IEEE Transactions on Biomedical Engineering*, vol. 56, pp. 2044-2053, Aug 2009.
- [5] B. R. Epstein and K. R. Foster, "Anisotropy in the dielectric-properties of skeletal-muscle," *Medical & Biological Engineering & Computing*, vol. 21, pp. 51-55, 1983 1983.
- [6] J. Baan, E. T. Vandervelde, H. G. Debruijn, G. J. Smeenk, J. Koops, A. K. Raghavan, D. Temmerman, J. Senden, and B. Buis, "Continuous Measurement of Left-Ventricular Volume in Animals and Humans by Conductance Catheter," *Circulation*, vol. 70, pp. 812-823, 1984.
- [7] J. E. Porterfield, A. T. G. Kottam, K. Raghavan, D. Escobedo, J. T. Jenkins, E. R. Larson, R. J. Trevino, J. W. Valvano, J. A. Pearce, and M. D. Feldman, "Dynamic correction for parallel conductance, $G(P)$, and gain factor, α , in invasive murine left ventricular volume measurements," *Journal of Applied Physiology*, vol. 107, pp. 1693-1703, Dec 2009.
- [8] S. Grimnes and O. G. Martinsen, "Sources of error in tetrapolar impedance measurements on biomaterials and other ionic conductors," *Journal of Physics D-Applied Physics*, vol. 40, pp. 9-14, Jan 7 2007.
- [9] D. Geselowitz, "Application of electrocardiographic lead theory to impedance plethysmography," *IEEE Transactions on Biomedical Engineering*, vol. BM18, pp. 38-&, 1971.
- [10] J. Lehr, "Vector derivation useful in impedance plethysmographic field calculations," *IEEE Transactions on Biomedical Engineering*, vol. BM19, pp. 156-157, 1972 1972.
- [11] J. Porterfield, "Admittance for the Early Detection of Heart Failure," Doctor of Philosophy, Electrical Engineering, The University of Texas at Austin, 2010.
- [12] M. D. Feldman, J. M. Erikson, Y. Mao, C. E. Korcarz, R. M. Lang, and G. L. Freeman, "Validation of a mouse conductance system to determine LV volume: comparison to echocardiography and crystals," *American Journal of Physiology-Heart and Circulatory Physiology*, vol. 279, pp. H1698-H1707, Oct 2000.
- [13] C. L. Wei, J. W. Valvano, M. D. Feldman, and J. A. Pearce, "Nonlinear conductance-volume relationship for murine conductance catheter measurement system," *IEEE Transactions on Biomedical Engineering*, vol. 52, pp. 1654-1661, Oct 2005.
- [14] X. M. Gao, A. M. Dart, E. Dewar, G. Jennings, and X. J. Du, "Serial

echocardiographic assessment of left ventricular dimensions and function after myocardial infarction in mice," *Cardiovascular Research*, vol. 45, pp. 330-338, Jan 14 2000.

- [15] S. Gabriel, R. W. Lau, and C. Gabriel, "The dielectric properties of biological tissues .2. Measurements in the frequency range 10 Hz to 20 GHz," *Physics in Medicine and Biology*, vol. 41, pp. 2251-2269, Nov 1996.
- [16] J. E. Porterfield, E. R. Larson, J. T. Jenkins, D. Escobedo, J. W. Valvano, J. A. Pearce, and M. D. Feldman, "Left ventricular epicardial admittance measurement for detection of acute LV dilation," *Journal of Applied Physiology*, vol. 110, pp. 799-806, Mar 2011.
- [17] C. Carlsson, E. Soderqvist, L. A. Brodin, G. Kallner, J. Hultman, H. Elmqvist, and S. Saha, "Initial experience with a thin single segment pressure and conductance catheter for measurement of left ventricular volume," in *23rd Annual International Conference of the IEEE-Engineering-in-Medicine-and-Biology-Society*, Istanbul, Turkey, 2001, pp. 103-106.



Erik R. Larson received his B.S.E.E, M.S.E., and Ph.D. degrees in electrical engineering from the University of Texas at Austin in 2006, 2008, and 2012 respectively. His dissertation focused on the admittance method for the determination of cardiac hemodynamics using biventricular pacing leads and conductance catheters.

He is currently a Research Engineer at Windmill Cardiovascular Systems, Austin, Texas.



Marc D. Feldman received the B.S. degree from Duke University, Durham, NC, in 1977, and the M.D. degree from the University of Pennsylvania School of Medicine, Philadelphia, in 1981.

He completed his internship and residency at Billings Hospital, University of Chicago, Chicago, IL. He was a Clinical and a Research Fellow in cardiology at Beth Israel Hospital,

Harvard Medical School, Boston, MA. He is currently a Professor of Medicine and Engineering, and the Director of the Cardiac Catheterization Laboratories, Division of Cardiology, The University of Texas Health Sciences Center at San Antonio. He is also an Adjunct Professor at The University of Texas at Austin.



Jonathan W. Valvano (M'83) was born in Clinton, CT, in 1953. He received the B.S. degree in computer science and engineering and the M.S. degree in electrical engineering and computer science from Massachusetts Institute of Technology (MIT), Cambridge, in 1977, and the Ph.D. degree in medical engineering from Harvard University/MIT Division of Health Sciences and Technology, Cambridge, in 1981.

He is currently a Full Professor at The University of Texas at Austin, where he is engaged in research in the fields of embedded systems, low-power medical electronics, and cardiac measurements.



John A. Pearce (S'79–M'80–SM'92) received the B.S.M.E. and the M.S.M.E. degrees from Clemson University, Clemson, SC, in 1968 and 1971, respectively, and the M.S.E.E. and Ph.D. degrees in electrical engineering from Purdue University, West Lafayette, IN, in 1977 and 1980, respectively.

In 1982, he joined the Faculty of Electrical and Computer Engineering, The University of Texas at Austin, where he is currently the Temple Foundation Professor (#3), the Department Undergraduate Adviser and the Adviser for the Biomedical Engineering Track in the Graduate Program. His current research interests include interactions between electromagnetic fields and tissues. He is also involved in the basic science of tissue ablation and thermal damage. He is currently investigating how the complex electrical properties of cardiac muscle can be applied to identify its contribution to the electrical admittance signal.

Dr. Pearce won the Presidential Young Investigator Award from the National Science Foundation in 1985.